

MSUHEP-040106  
hep-ph/0401026

# Combined Effect of QCD Resummation and QED Radiative Correction to $W$ boson Observables at the Tevatron

Qing-Hong Cao\* and C.-P. Yuan†

*Department of Physics & Astronomy,  
Michigan State University,  
East Lansing, MI 48824, USA.*

## Abstract

A precise determination of the  $W$  boson mass at the Fermilab Tevatron requires a theoretical calculation in which the effects of the initial-state multiple soft-gluon emission and the final-state photonic correction are simultaneously included. Here, we present such a calculation and discuss its prediction on the transverse mass distribution of the  $W$  boson and the transverse momentum distribution of its decay charged lepton, which are the most relevant observables for measuring the  $W$  boson mass at hadron colliders.

---

\*Electronic address: cao@pa.msu.edu

†Electronic address: yuan@pa.msu.edu

As a fundamental parameter of the Standard Model (SM), the mass of the  $W$ -boson ( $M_W$ ) is of particular importance. Aside from being an important test of the SM itself, a precision measurement of  $M_W$ , together with an improved measurement of top quark mass ( $M_t$ ), provides severe indirect bounds on the mass of Higgs boson ( $M_H$ ). With a precision of 27 MeV for  $M_W$  and 2.7 GeV for  $M_t$ , which are the target values for Run II of the Fermilab Tevatron collider,  $M_H$  in the SM can be predicted with an uncertainty of about 35% [1]. Comparison of these indirect constraints on  $M_H$  with the results from direct Higgs boson searches, at the LEP2, the Tevatron and the CERN Large Hadron Collider (LHC), will be an important test of the SM. In order to have a precision measurement of  $M_W$ , the theoretical uncertainties, dominantly coming from the transverse momentum of the  $W$ -boson ( $P_T^W$ ), the uncertainty in parton distribution function (PDF) and the electroweak (EW) radiative corrections to the  $W$  boson decay, must be controlled to a better accuracy [3].

At the Tevatron, about ninety percent of the production cross section of  $W$  boson is in the small transverse momentum region, where  $P_T^W \leq 20$  GeV. When  $P_T^W$  is much smaller than  $M_W$ , every soft-gluon emission will induce a large logarithmic contribution to the  $P_T^W$  distribution so that the order-by-order perturbative calculation in the theory of Quantum chromodynamics (QCD) cannot accurately describe the  $P_T^W$  spectrum and the contribution from multiple soft-gluon emission, which contributes to all orders in the expansion of the strong coupling constant  $\alpha_s$ , needs to be summed to all orders. It has been shown that by applying the renormalization group analysis, the multiple soft-gluon radiation effects can be resummed to all orders to predict the  $P_T^W$  distribution that agrees with experimental data [4, 5]. RESBOS, a Monte Carlo (MC) program [5] resumming the initial-state soft-gluon radiations of the hadronically produced lepton pairs through EW vector boson production and decay at hadron colliders  $p\bar{p}/pp \rightarrow V(\rightarrow \ell_1\bar{\ell}_2)X$ , has been used by the CDF and DØ Collaborations at the Tevatron to compare with their data in order to determine  $M_W$ . However, RESBOS does not include any higher order EW corrections to describe the vector boson decay. The EW radiative correction, in particular the final-state QED correction, is crucial for precision measurement of  $W$  boson mass at the Tevatron, because photon emission from the final-state charged lepton can significantly modify the lepton momentum which is used in the determination of  $M_W$ . In the CDF Run Ib  $W$  mass measurement, the mass shifts due to radiative effects were estimated to be  $-65 \pm 20$  MeV and  $-168 \pm 10$  MeV for the electron and muon channels, respectively [2]. The full next-to-leading order (NLO)  $O(\alpha)$  EW corrections have been calculated [8, 9] and resulted in WGRAD [9], a MC program for calculating  $O(\alpha)$  EW ra-

diative corrections to the process  $p\bar{p} \rightarrow \nu_\ell \ell(\gamma)$ . However, WGRAD does not include the dominant correction originated from the initial-state multiple soft-gluon emission. To incorporate both the initial-state QCD and final-state QED corrections into a parton level MC program is urgently required to reduce the theoretical uncertainties in interpreting the experimental data at the Tevatron. It was shown in Refs. [8, 9] that at the NLO, the EW radiative correction in  $p\bar{p} \rightarrow \ell\nu_\ell(\gamma)$  is dominated by the final-state QED (FQED) correction. Hence, in this paper we present a consistent calculation which includes both the initial-state multiple soft-gluon QCD resummation and the final-state NLO QED corrections, and develop an upgraded version of the RESBOS program, called RESBOS-A [10], to simulate the signal events.

The fully differential cross section for the production and decay of the  $W$  boson that includes only the effect of the initial-state multiple QCD soft-gluon emission can be found in Ref. [5]. To include also the final-state NLO QED contributions, we sum up the following two sets of differential cross sections. One, cf. Eq. (1), contains final-state QED virtual correction and part of the real photon emission contribution in which photon is either soft or collinear. Another, cf. Eq. (2), includes the hard photon contribution from the real photon emission processes. Denote  $Q$ ,  $y$ ,  $Q_T$  and  $\phi_W$  to be the invariant mass, rapidity, transverse momentum and azimuthal angle of the di-lepton pair, respectively. For  $W^+$  production and decay, we have

$$\begin{aligned} & \left( \frac{d\sigma(h_1 h_2 \rightarrow W^+ (\rightarrow \nu_\ell \ell^+(\gamma)) X)}{dQ^2 dy dQ_T^2 d\phi_W d\Pi_2} \right)_{\text{res}} \\ &= \frac{1}{48\pi S} \left\{ \frac{1}{(2\pi)^2} \int d^2 b e^{i\vec{Q}_T \cdot \vec{b}} \times \sum \widetilde{W}_{j\bar{k}}^{(2)}(b_*, Q, x_1, x_2, C_1, C_2, C_3) \widetilde{W}_{j\bar{k}}^{\text{NP}}(b, Q, x_1, x_2) \right. \\ & \quad \left. + Y(Q_T, Q, x_1, x_2, C_4) \right\}, \end{aligned} \quad (1)$$

and

$$\begin{aligned} & \left( \frac{d\sigma(h_1 h_2 \rightarrow W^+ (\rightarrow \nu_\ell \ell^+\gamma) X)}{dQ^2 dy dQ_T^2 d\phi_W d\Pi_3} \right)_{\text{res}} \\ &= \frac{1}{48\pi S} \left\{ \frac{1}{(2\pi)^2} \int d^2 b e^{i\vec{Q}_T \cdot \vec{b}} \times \sum \widetilde{W}_{j\bar{k}}^{(3)}(b_*, Q, x_1, x_2, C_1, C_2, C_3) \widetilde{W}_{j\bar{k}}^{\text{NP}}(b, Q, x_1, x_2) \right\}, \end{aligned} \quad (2)$$

where  $d\Pi_2$  and  $d\Pi_3$  represents the two-body and three-body phase space of the vector boson decay products, respectively. In the above equations the parton momentum fractions are defined as  $x_1 = \frac{Q e^y}{\sqrt{S}}$  and  $x_2 = \frac{Q e^{-y}}{\sqrt{S}}$ , where  $\sqrt{S}$  is the center-of-mass energy of the hadrons  $h_1$  and  $h_2$ .

The renormalization group invariant quantities  $\widetilde{W}_{j\bar{k}}^{(2)}(b)$  and  $\widetilde{W}_{j\bar{k}}^{(3)}(b)$ , which sum to all orders in  $\alpha_S$  all the singular terms that behave as  $Q_T^{-2} \times [1 \text{ or } \ln(Q_T^2/Q^2)]$  for  $Q_T \rightarrow 0$ , are

$$\begin{aligned} & \widetilde{W}_{j\bar{k}}^{(2)}(b, Q, x_1, x_2, C_1, C_2, C_3) \\ &= e^{-S(b, Q, C_1, C_2)} |V_{jk}|^2 \times \left\{ \left[ (C_{ja} \otimes f_{a/h_1})(x_1) (C_{\bar{k}b} \otimes f_{b/h_2})(x_2) + (x_1 \leftrightarrow x_2) \right] \right. \\ & \quad \left. \times \frac{d\hat{\sigma}_F^{(0+1)}}{d\Pi_2}(j\bar{k} \rightarrow \nu_\ell \ell^+(\gamma)) \right\}, \end{aligned} \quad (3)$$

and

$$\begin{aligned} & \widetilde{W}_{j\bar{k}}^{(3)}(b, Q, x_1, x_2, C_1, C_2, C_3) \\ &= e^{-S(b, Q, C_1, C_2)} |V_{jk}|^2 \times \left\{ \left[ (C_{ja} \otimes f_{a/h_1})(x_1) (C_{\bar{k}b} \otimes f_{b/h_2})(x_2) + (x_1 \leftrightarrow x_2) \right] \right. \\ & \quad \left. \times \frac{d\hat{\sigma}_F^{(1)}}{d\Pi_3}(j\bar{k} \rightarrow \nu_\ell \ell^+\gamma) \right\}, \end{aligned} \quad (4)$$

where  $\hat{\sigma}_F^{(0)}$  is the Born level parton cross section for  $j\bar{k} \rightarrow \nu_\ell \ell^+$ , and  $\hat{\sigma}_F^{(1)}$  includes the final-state NLO QED corrections. The notation  $\otimes$  denotes the convolution [5]

$$(C_{ja} \otimes f_{a/h_1})(x_1) = \int_{x_1}^1 \frac{d\xi_1}{\xi_1} C_{ja} \left( \frac{x_1}{\xi_1}, b, \mu = \frac{C_3}{b}, C_1, C_2 \right) \times f_{a/h_1} \left( \xi_1, \mu = \frac{C_3}{b} \right), \quad (5)$$

and the  $V_{jk}$  coefficients are the Cabibbo-Kobayashi-Maskawa mixing matrix elements. In the above expression  $j$  represents quark flavors and  $\bar{k}$  stands for antiquark flavors. The indices  $a$  and  $b$  are meant to sum over quarks and antiquarks or gluons. Summation on these double indices is implied. As compared to the results shown in Refs. [4, 5],  $\widetilde{W}_{j\bar{k}}^{(2)}(b)$  and  $\widetilde{W}_{j\bar{k}}^{(3)}(b)$  contain additional  $\frac{\alpha}{\pi}$  corrections, which come from the final state QED corrections. The Sudakov exponent  $S(b, Q, C_1, C_2)$  in Eqs. (3) and (4) is defined as [5]

$$S(b, Q, C_1 C_2) = \int_{C_1^2/b^2}^{C_2^2 Q^2} \frac{d\bar{\mu}^2}{\bar{\mu}^2} \left[ A(\alpha_S(\bar{\mu})) \ln \left( \frac{C_2^2 Q^2}{\bar{\mu}^2} \right) + B(\alpha_S(\bar{\mu}), C_1, C_2) \right]. \quad (6)$$

The explicit forms of the  $A$ ,  $B$ , and  $C_{ja}$  functions and the renormalization constants  $C_i$  ( $i = 1, 2, 3$ ) can be found in Appendix D of Ref. [5]. In our calculation, we have included  $A^{(1)}, A^{(2)}, B^{(1)}, B^{(2)}$ ,  $C^{(0)}$  and  $C^{(1)}$ , with canonical choice of  $C_i$ 's. The  $Y$  piece in Eq. (1), which is the difference of the fixed order perturbative result and their singular part, can be found in Appendix E of Ref. [5].

We follow the prescription in Ref. [7], which decomposes the electroweak  $O(\alpha)$  contribution to the resonant single  $W$  production in a general 4-fermion process into gauge invariant QED-like

and weak parts, to extract a gauge invariant QED-like form factor from the photon contribution. The NLO FQED differential cross sections are calculated by using phase space slicing method [6], which introduces two theoretical cutoff parameters, soft cutoff  $\delta_S$  and collinear cutoff  $\delta_C$ , to isolate the soft and collinear singularities associated with the real photon emission subprocesses by partitioning phase space into soft, collinear and hard regions such that

$$|\mathcal{M}^r|^2 = |\mathcal{M}^r|_{\text{soft}}^2 + |\mathcal{M}^r|_{\text{collinear}}^2 + |\mathcal{M}^r|_{\text{hard}}^2. \quad (7)$$

The soft region is thus defined by requiring that the photon energy ( $E_\gamma$ ) in the ( $j\bar{k}$ ) parton center-of-mass frame to satisfy  $E_\gamma < \delta_S \sqrt{\hat{s}}/2$ , where  $\sqrt{\hat{s}}$  is the invariant mass of the ( $j\bar{k}$ ) partons. Using the dimensional regularization scheme, we can then evaluate, in n-dimensions, the real photon emission diagrams under the soft photon approximation, where the photon momentum is set to be zero in the numerator, and integrate over the soft region. In the soft and collinear regions the cross section is proportional to the Born cross section. The soft singularities originating from the final-state photon radiation cancel against the corresponding singularities from the final-state virtual corrections and leave a finite result depending on the soft cutoff parameter  $\delta_S$ . For  $E_\gamma > \delta_S \sqrt{\hat{s}}/2$ , the real photon emission diagrams are calculated in four dimensions using the helicity amplitude method. The collinear singularities associated with photon radiation from the final-state charged lepton is regulated by the finite lepton mass. The end result of the calculation consists of two sets of weighted events corresponding to the  $j\bar{k} \rightarrow \nu_\ell \ell^+(\gamma)$  and  $j\bar{k} \rightarrow \nu_\ell \ell^+ \gamma$  contributions which are included in Eqs. (1) and (2), separately. Each set depends on the soft cutoff parameter  $\delta_S$ . The sum of the two contributions, however, is independent of  $\delta_S$ , as long as the soft cutoff is small enough to validate the soft-gluon approximation. In our numerical studies, we take  $\delta_S = 0.001$  which yields a stable numerical result in agreement with Refs. [8, 9]. Through our calculation, we adopt the CERN LEP line-shape prescription of a resonance state and write the  $W$  boson propagator as

$$\frac{1}{(p^2 - M_W^2) + iM_W \Gamma_W p^2/M_W^2}, \quad (8)$$

where  $\Gamma_W$  is the width of  $W$  boson.

To examine how much the combined contributions from the initial-state QCD resummation and the final-state QED corrections can affect the precision measurement of  $M_W$ , we perform Monte Carlo analyses to study a few experimental observables that are most sensitive to the measurement of  $M_W$  at the Tevatron (a  $p\bar{p}$  collider with  $\sqrt{S}=1.96$  TeV). For the numerical evaluation we chose the following set of SM parameters:  $\alpha = 1/137.0359895$ ,  $G_\mu = 1.16637 \times 10^{-5} \text{GeV}^{-2}$ ,  $M_W =$

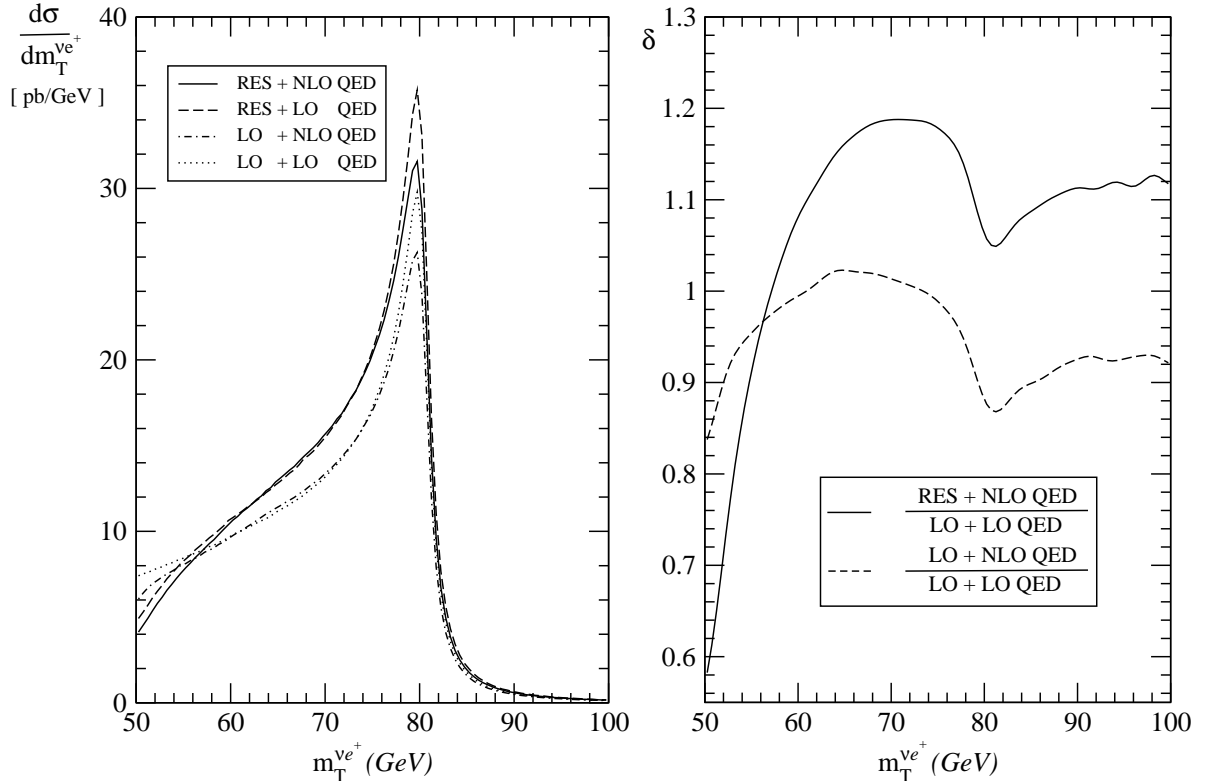


FIG. 1: Transverse mass distribution of  $W^+$  boson

$80.35 \text{ GeV}$ ,  $\Gamma_W = 2.0887 \text{ GeV}$ ,  $M_Z = 91.1867 \text{ GeV}$ ,  $m_e = 0.51099907 \text{ MeV}$ . Thus, the square of the weak gauge coupling is  $g^2 = 4\sqrt{2}M_W^2 G_\mu$ . Because of the limited space, we focus our attention on the positively charged electron lepton (i.e. positron) only, though our analysis procedure also applies to the  $\mu$  lepton. The complete study including both electron and muon leptons will be shown in our forthcoming paper, in which we also extend our study to the LHC.

The  $W$  events in these analyses are selected by demanding a single isolated high  $p_T$  charged lepton in conjunction with large missing transverse energy. To model the acceptance cuts used by the CDF and DØ Collaborations in their  $W$  mass analyses, we impose the following transverse momentum ( $p_T$ ) and pseudo-rapidity ( $\eta$ ) cuts on the final-state leptons:

$$p_T^e > 25 \text{ GeV}, |\eta(e)| < 1.2, \cancel{E}_T > 25 \text{ GeV}. \quad (9)$$

Due to the overwhelming QCD backgrounds, the measurement of  $W$  boson mass at hadron collider is performed in the leptonic decay channels. Since the longitudinal momentum of the neutrinos produced in the leptonic  $W$  boson decays ( $W^+ \rightarrow \nu_e e^+$ ) cannot be measured, there is insufficient information to reconstruct the invariant mass of the  $W$  boson. Instead, the transverse mass distribution of the final state lepton pair, which exhibits a Jacobian edge at  $M_T \sim M_W$ , is

used to extract out  $M_W$ . Transverse mass ( $M_T^W$ ) of  $W$  is defined as

$$M_T^W = \sqrt{2p_T^e p_T^\nu (1 - \cos \phi)}, \quad (10)$$

where  $\phi$  is the angle between the charged lepton and the neutrino in the transverse plane. The neutrino transverse momentum ( $p_T^\nu$ ) is identified with the missing transverse energy ( $E_T$ ) in the event. In Fig. 1, we show various theory predictions on the  $M_T^W$  distribution. The legend of the figure is defined as follows:

- LO : including only the Born level initial-state contribution,
- RES : including the initial-state multiple soft-gluon corrections via QCD resummation,
- LO QED : including only the Born level final-state contribution,
- NLO QED : including the final-state NLO QED corrections.

For example, the solid curve (labelled as RES+NLO QED) in Fig. 1(a) is the prediction from our combined calculation given by Eqs. (1) and (2).

As shown in Fig. 1(a), compared to the lowest order cross section (dotted curve), the initial state QCD resummation effects (dashed curve) increase the cross section at the peak of the  $M_T^W$  distribution by about 20%, and the final state NLO QED corrections (dot-dashed curve) decrease it by about  $-12\%$ , while the combined contributions (solid curve) of the QCD resummation and FQED corrections increase it by 7%. In addition to the change in magnitude, the line-shape of the  $M_T^W$  distribution is significantly modified by the effects of QCD resummation and FQED corrections. To illustrate this point, we plot the ratio of the (RES+NLO QED) differential cross sections to the LO ones as the solid curve in Fig. 1(b). The dashed curve is for the ratio of (LO+NLO QED) to LO. As shown in the figure, the QCD resummation effect dominates the shape of  $M_T^W$  distribution for  $65 \text{ GeV} \leq M_W \leq 95 \text{ GeV}$ , while the FQED correction reaches its maximal effect around the Jacobian peak ( $M_T^W \simeq M_W$ ). Hence, both corrections must be included to accurately predict the distribution of  $M_T^W$  around the Jacobian region to determine  $M_W$ . We note that after including the effect due to the finite resolution of the detector (for identifying an isolated electron or muon), the size of the FQED correction is largely reduced [8, 9].

Although the  $M_T^W$  distribution has been the optimal observable for determining  $M_W$  at the Tevatron, it requires an accurate measurement of the missing transverse momentum direction which is in practice difficult to control. On the other hand, the transverse momentum of the decay

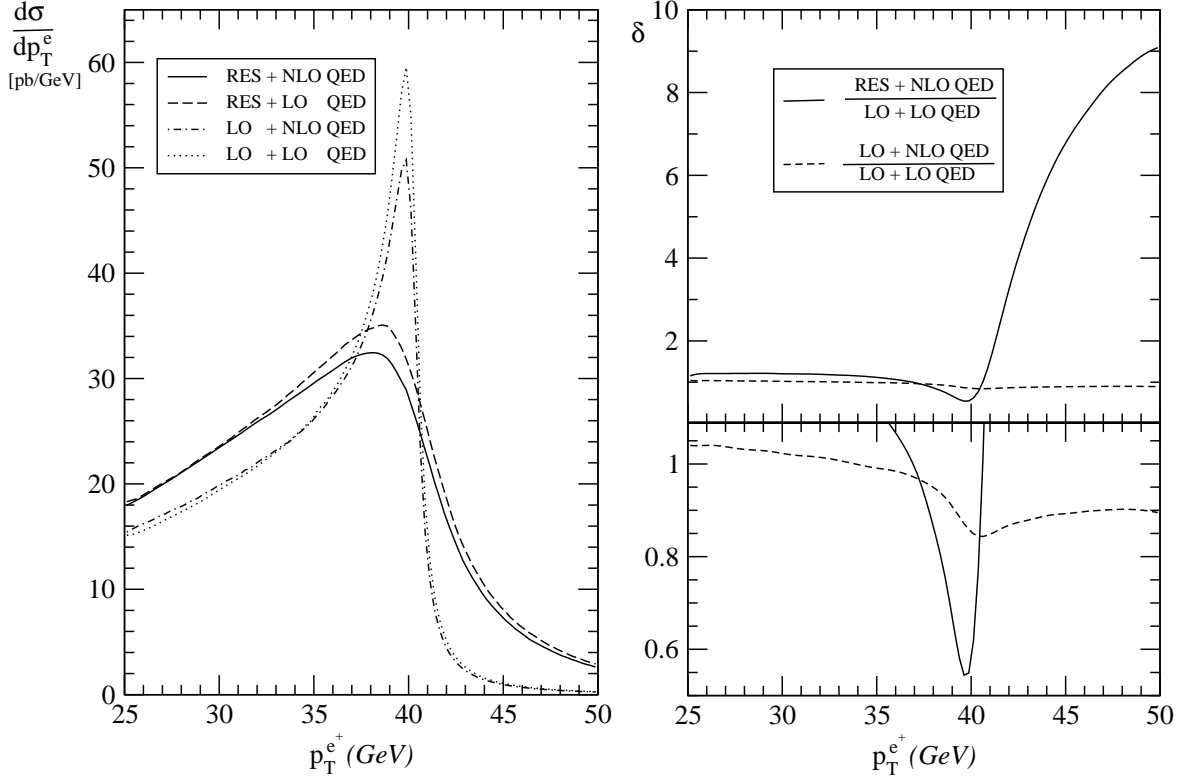


FIG. 2: Transverse momentum distributions of  $e^+$

charged lepton ( $p_T^e$ ) is less sensitive to the detector resolution, so that it can be used to measure  $M_W$  and provide important cross-check on the result derived from the  $M_T^W$  distribution, for they have different systematic uncertainties. Another important feature of this observable is that  $p_T^e$  distribution is more sensitive to the transverse momentum of  $W$  boson. Hence, the QCD soft-gluon resummation effects, the major source of  $p_T^W$ , must be included to reduce the theoretical uncertainty of this method. In Fig. 2(a), we show the  $p_T^e$  distributions predicted by various theory calculations, and in Fig. 2(b), the ratios of the higher order to lowest order cross sections as a function of  $p_T^e$ . The lowest order distribution (dotted curve) shows a clear and sharp Jacobian peak at  $p_T^e \simeq M_W/2$ , and the distribution with the NLO final-state QED correction (dot-dashed curve) also exhibits the similar Jacobian peak with the peak magnitude reduced by about 15%. But the clear and sharp Jacobian peak of the lowest order and NLO FQED distributions (in which  $p_T^W = 0$ ) are strongly smeared by the finite transverse momentum of the  $W$  boson induced by multiple soft-gluon radiation, as clearly demonstrated by the QCD resummation distribution (dashed curve) and the combined contributions of the QCD resummation and FQED corrections (solid curve). Similar to the  $M_T^W$  distribution, the QCD resummation effect dominates the whole  $p_T^e$  range, while

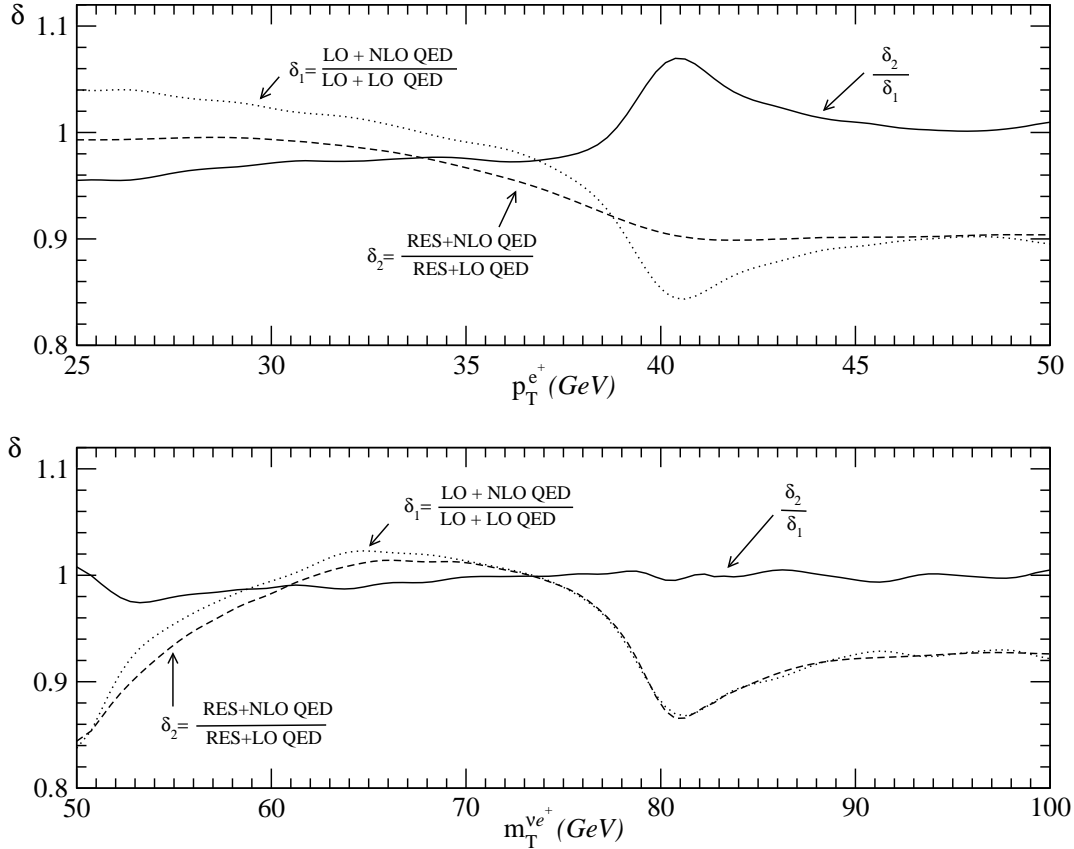


FIG. 3: Distributions of  $\mathcal{R}$ ,  $\delta_1$  and  $\delta_2$

the FQED correction reaches its maximum around the Jacobian peak (half of  $M_W$ ). The combined contribution of the QCD resummation and FQED corrections reaches the order of 45% near the Jacobian peak. Hence, these lead us to conclude that the QCD resummation effects are crucial in the measurement of  $M_W$  from fitting the Jacobian kinematical edge of the  $p_T^e$  distribution.

It is also interesting to examine the effect of the final-state NLO QED correction to the theory predictions with LO (leading order) or RES (resummed) initial-state cross sections, which is described by the observable  $\mathcal{R}$ , defined as

$$\mathcal{R} = \frac{\delta_2}{\delta_1}, \quad (11)$$

where

$$\begin{aligned} \delta_1 &= \frac{\text{LO + NLO QED}}{\text{LO + LO QED}}, \\ \delta_2 &= \frac{\text{RES + NLO QED}}{\text{RES + LO QED}}. \end{aligned} \quad (12)$$

The distributions of  $\mathcal{R}$  as a function of  $p_T^e$  and  $M_T^W$  are shown in the upper part and lower part of

Fig. 3, respectively. As expected, the  $\mathcal{R}(M_T)$  distribution is almost flat all the way from 60 GeV to 100 GeV, but the  $\mathcal{R}(p_T^e)$  distribution deviates from one in the Jacobian peak region. This is due to the fact that  $p_T^e$  is more sensitive to  $P_T^W$  than  $M_T^W$ .

In order to study the impact of the presented calculation to the determination of the  $W$  boson mass, the effect due to the finite resolution of the detector should be included, which will be presented elsewhere.

We thank P. Nadolsky and J.W. Qiu for helpful discussions. This work was supported in part by NSF under grand No. PHY-0244919 and PHY-0100677.

- [1] U. Baur, R. Clare, J. Erler, S. Heinemeyer, D. Wackerlo, G. Weiglein and D. R. Wood, in *Proc. of the APS/DPF/DPB Summer Study on the Future of Particle Physics (Snowmass 2001)* ed. N. Graf, eConf **C010630**, P122 (2001) [arXiv:hep-ph/0111314].
- [2] T. Affolder *et al.* [CDF Collaboration], Phys. Rev. D **64**, 052001 (2001) [arXiv:hep-ex/0007044].
- [3] U. Baur, R. K. Ellis and D. Zeppenfeld, FERMILAB-PUB-00-297 *Prepared for Physics at Run II: QCD and Weak Boson Physics Workshop: Final General Meeting, Batavia, Illinois, 4-6 Nov 1999*
- [4] C. Balazs, J. W. Qiu and C.-P. Yuan, Phys. Lett. B **355**, 548 (1995) [arXiv:hep-ph/9505203].
- [5] C. Balazs and C.-P. Yuan, Phys. Rev. D **56**, 5558 (1997) [arXiv:hep-ph/9704258].
- [6] H. Baer, J. Ohnemus and J. F. Owens, Phys. Rev. D **40**, 2844 (1989).
- [7] D. Wackerlo and W. Hollik, Phys. Rev. D **55**, 6788 (1997) [arXiv:hep-ph/9606398].
- [8] S. Dittmaier and M. Kramer, Phys. Rev. D **65**, 073007 (2002) [arXiv:hep-ph/0109062].
- [9] U. Baur, S. Keller and D. Wackerlo, Phys. Rev. D **59**, 013002 (1999) [arXiv:hep-ph/9807417].
- [10] A Fortran code that implements the theoretical calculation presented in this work.